

Informative Path Planning for Active Mapping under Localization Uncertainty

Marija Popović, Teresa Vidal-Calleja, Jen Jen Chung, Juan Nieto, Roland Siegwart

Abstract— **I**nformation gathering algorithms play a key role in unlocking the potential of robots for efficient data collection in a wide range of applications. However, most existing strategies neglect the fundamental problem of the robot pose uncertainty, which is an implicit requirement for creating robust, high-quality maps. To address this issue, we introduce an informative planning framework for active mapping that explicitly accounts for the pose uncertainty in *both* the mapping and planning tasks. Our strategy exploits a Gaussian Process (GP) model to capture a target environmental field given the uncertainty on its inputs. For planning, we formulate a new utility function that couples the localization and field mapping objectives in GP-based mapping scenarios in a principled way, without relying on any manually tuned parameters. Extensive simulations show that our approach outperforms existing strategies, with reductions of up to 45.1% and 6.3% in mean pose uncertainty and map error. We also present a proof of concept in an indoor temperature mapping scenario.

I. INTRODUCTION

Rapid technological advancements are inciting the use of autonomous mobile robots for exploration and data acquisition. In many marine [1, 2], terrestrial [3, 4], and airborne [5, 6] applications, these systems have the ability to bridge the spatiotemporal divides limiting traditional measurement methods in a safer and more cost-effective manner [7]. However, to fully exploit their potential, algorithms are required for planning efficient informative paths in complex environments under platform-specific constraints.

This paper examines the problem of active mapping using a robot, where the aim is to recover a continuous 2-D or 3-D field, e.g., of temperature, humidity, etc., using measurements collected by an on-board sensor. In similar setups, most existing strategies [1, 5, 8] incorrectly assume perfect pose information, which is an implicit requirement for building high-quality maps in initially unknown environments. Our motivation is to improve upon the robustness and accuracy of field reconstructions by allowing the robot to adaptively trade-off between gathering new information (exploration) and maintaining good localization (exploitation).

Despite recent efforts [2, 6, 9, 10], propagating both the localization and field map uncertainties into the planning framework in a principled manner remains an open challenge. A major issue arises due to the different ways in which the target field and robot pose are modeled. In particular, our work considers the task of mapping a field using a

M. Popović, J. J. Chung, J. Nieto, and R. Siegwart are with the Autonomous Systems Lab., ETH Zürich, Zürich, Switzerland. T. Vidal-Calleja is with the Centre for Autonomous Systems at the Faculty of Engineering and IT, University of Technology Sydney, Australia. Corresponding author: mpopovic@ethz.ch.

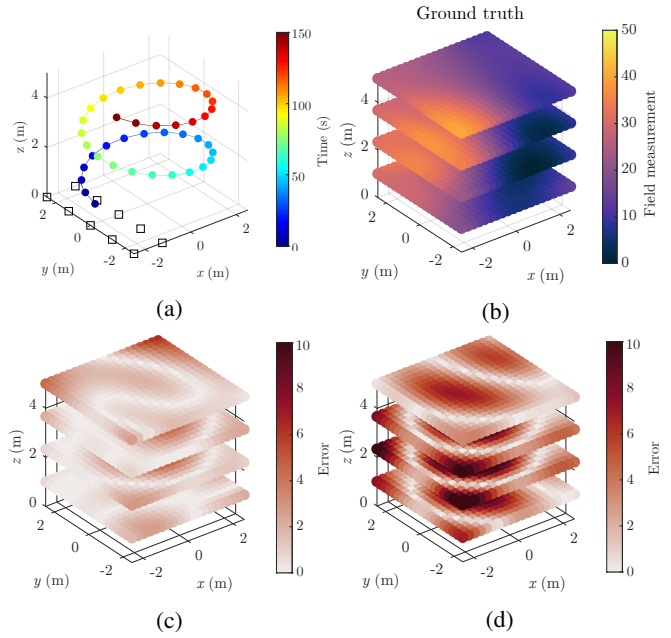


Fig. 1: Overview of our proposed active mapping strategy. (a) shows a spiral trajectory traveled by a robot. The squares indicate point landmarks on the ground used for localization. The spheres represent sites where measurements of the ground truth field map in (b) are taken. By accounting for pose estimation uncertainty, our framework yields an error map (c) with 2.47 times lower total error compared to a standard mapping approach (d).

Gaussian Process (GP) with the robot pose represented as a multivariate Gaussian distribution. In this setup, measures of uncertainty in the field and robot pose, e.g., entropy-based criteria [4], are not directly comparable since they are obtained from their respective model variances which have different units and scales, and are therefore difficult to couple in a single utility function for multi-objective planning. Heuristic methods, e.g., based on a linear weighting of uncertainties [11], are commonly applied; however, they require careful manual tuning and are often scenario-specific.

To address this, we present an approach that accounts for the pose estimation uncertainty in two places. First, we consider the additional noise the pose uncertainty induces in the environmental field model; second, we include it as a shaping factor in the utility function that defines our informative planning task. Our mapping strategy uses GPs with uncertain inputs (UIs) [2] to propagate the pose uncertainty into the field model. During a mission, the map built online is used to plan informative trajectories in continuous space by optimizing initial solutions obtained by a coarse grid

search. We develop a new utility formulation for GP-based mapping scenarios that jointly considers the uncertainty of the robot and the field models. This enables us to capture the desired exploitation-exploration trade-off in a mathematically sound manner, without relying on any manually-tuned, environment-dependent parameters. In summary, the contributions of this work are:

- 1) A utility function based on GP field models that tightly couples the objectives of robot localization and field mapping in active mapping problems.
- 2) An informative planning framework that accounts for the pose uncertainty in both mapping and the information objective for planning.
- 3) Evaluations of the approach in a 3-D graph Simultaneous Localization and Mapping (SLAM) setup and a proof of concept in a temperature mapping scenario.

We note that our framework can be used in any scalar field mapping scenario, e.g., spatial occupancy [4, 6, 12], signal strength [2, 8], aerial surveillance [5, 7], etc., and with any SLAM or localization-only back end. Moreover, the applicability of our utility function extends to other areas of robotics, such as reinforcement learning [13].

II. RELATED WORK

Significant recent work has been done on autonomous data gathering strategies in the context of robotics and related fields. The discussion in this section focuses on two main research streams: (1) methods for probabilistic environmental mapping [2, 6, 9, 14], and (2) algorithms for informative planning [1, 4, 5, 12, 15, 16].

GPs are a popular non-parameteric Bayesian technique for modeling spatio-temporal phenomena [14]. They have been applied in various active sensing scenarios [1, 3, 5, 16] to gather data based on correlations and uncertainty in continuous maps. However, most of these works assume that the training data for prediction is inherently noise-free, which may lead to inaccuracies if measurements are incorporated at wrong locations and mislead predictive planning algorithms.

Propagating the input uncertainty through dense GP models is a computationally challenging task. To address this, analytical [9] and heteroscedastic approximation methods [2, 3, 10] have been proposed. Our work leverages the expected kernel technique of Jadidi et al. [2] by integrating over UIs with deterministic query points. Specifically, we extend their approach to more complex planning problems in 3-D scenarios, and integrate it with a new uncertainty-aware utility function. This coupling enables robust, tractable mapping under robot pose uncertainty for online sensing applications.

An active sensing task can be expressed in a Partially Observable Markov Decision Process (POMDP) [17] as one of decision-making under uncertainty. In practice, informative planning algorithms are typically used to render this problem computationally tractable with dense belief representations. We broadly distinguish between planning strategies operating in (a) discrete [4, 12] and (b) continuous space. This study focuses on the latter class of methods, which leverage incremental sampling [6, 8, 18, 19] or splines [1, 5] to offer

greater scalability compared to discrete approaches. As in our prior work [5, 15, 16], we define smooth polynomial robot trajectories [20] and optimize them globally for an information objective in a finite-horizon manner.

Relatively limited research has been invested in active sensing scenarios where robot localization is uncertain. This setup has been tackled in the contexts of belief-space planning [6, 18, 19] and active SLAM [11, 12], where the aim is to maintain good localization as an unknown environment is explored. In contrast, and similarly to Papachristos et al. [6] and Costante et al. [18], our paper considers a setting where the map building and robot localization problems are decoupled. An important distinction is that we aim to reconstruct a continuous field that is independent of the environmental features used for localization.

An open challenge in this setup is formulating utility functions to trade off between robot localization and field mapping in a principled manner. To address this, previous approaches have examined heuristic parameter tuning [12], e.g., using a weighted linear combination of the map and pose uncertainties [11], and multi-layer [6, 18] planning strategies. In contrast to these methods, we follow Carrillo et al. [4] in using the concept of Rényi's entropy to discount information gain based on predicted localization uncertainty. Thereby, our utility function shares the benefit of coupling the two objectives in a mathematically sound way, without manual tuning requirements. The core difference is that our formulation is developed for a continuous mapping scenario based on a GP field model, instead of an occupancy grid. Moreover, by mapping with UIs, we present a unified framework where the robot localization uncertainty is jointly accounted for in *both* mapping and planning to achieve more robust data acquisition.

III. PROBLEM STATEMENT

The general active mapping problem is formulated as follows. We seek an optimal trajectory ψ^* in the space of all continuous trajectories Ψ to maximize an information-theoretic measure:

$$\begin{aligned} \psi^* = \operatorname{argmax}_{\psi \in \Psi} I(\operatorname{MEASURE}(\psi)), \\ \text{s.t. } \operatorname{COST}(\psi) \leq B. \end{aligned} \quad (1)$$

The function $\operatorname{MEASURE}(\cdot)$ obtains a finite set of measurements along trajectory ψ , and $\operatorname{COST}(\cdot)$ provides its associated cost, which cannot exceed a predefined budget B . The operator $I(\cdot)$ defines the information objective quantifying the utility of the acquired sensor measurements. In [Section V-C](#), we propose a utility function for active mapping in GP-based scenarios that incorporates both the robot localization and field mapping objectives without any manual parameter tuning requirements.

IV. MAPPING APPROACH

This section presents our mapping approach as the basis of our framework. We first describe our method for environmental field modeling using a GP, then present a strategy which folds the robot pose uncertainty into the map inference.

A. Gaussian Processes

We use a GP to model spatial correlations in a probabilistic and non-parametric manner [14]. The target field variable for mapping is assumed to be a continuous function: $f : \mathcal{E} \rightarrow \mathbb{R}$. A Gaussian correlated prior is placed over the function space, which is fully characterized by the mean function $m(\mathbf{x}) \triangleq \mathbb{E}[f(\mathbf{x})]$ and covariance function $k(\mathbf{x}, \mathbf{x}') \triangleq \mathbb{E}[(f(\mathbf{x}) - m(\mathbf{x}))(f(\mathbf{x}') - m(\mathbf{x}'))]$ as $f(\mathbf{x}) \sim \mathcal{GP}(m(\mathbf{x}), k(\mathbf{x}, \mathbf{x}'))$, where $\mathbb{E}[\cdot]$ is the expectation operator and \mathbf{x} and \mathbf{x}' are input vectors composed of spatial co-ordinates in the environment.

Let $\mathbf{x}_i \subset \mathcal{E}$ be a set of n observed input training points in the fixed-size environment with associated target values y_i . For a set of n^* query points $\mathbf{x}_{*i} \subset \mathcal{E}$, we can evaluate the predictive conditional Gaussian distribution $\mathbf{f}_* | \mathbf{X}, \mathbf{y}, \mathbf{X}_* \sim \mathcal{N}(\boldsymbol{\mu}, \mathbf{P})$ as follows [14]:

$$\boldsymbol{\mu} = m(\mathbf{X}_*) + K(\mathbf{X}_*, \mathbf{X}) [K(\mathbf{X}, \mathbf{X}) + \sigma_n^2 \mathbf{I}]^{-1} \times (\mathbf{y} - m(\mathbf{X})), \quad (2)$$

$$\mathbf{P} = K(\mathbf{X}_*, \mathbf{X}_*) - K(\mathbf{X}_*, \mathbf{X}) [K(\mathbf{X}, \mathbf{X}) + \sigma_n^2 \mathbf{I}]^{-1} \times K(\mathbf{X}_*, \mathbf{X})^\top, \quad (3)$$

where σ_n^2 is a hyperparameter representing the observation noise variance, $K(\mathbf{X}_*, \mathbf{X})$ denotes the cross-correlation terms between the query and observed points, and $K(\mathbf{X}, \mathbf{X})$ and $K(\mathbf{X}_*, \mathbf{X}_*)$ are the joint covariance matrices for the observed and query points, respectively. Note that $K(\cdot, \cdot)$ corresponds to the covariance function $k(\cdot, \cdot)$ for only one element.

B. Mapping Under Pose Uncertainty

To propagate the robot pose uncertainty into our mapping framework, we extend the expected kernel technique of Jaddidi et al. [2] to planning problems in 3-D setups. The key idea lies in taking the expectation of the covariance function k over UIs. Let $X \in \mathcal{X}$ be a random variable distributed according to a probability distribution $p(x)$. The expected covariance function \tilde{k} can be computed as:

$$\tilde{k} = \mathbb{E}[k] = \int_X kp(x)dx. \quad (4)$$

Assuming a Gaussian distribution for the robot pose $\mathcal{N}(\mathbf{p}, \Sigma)$, we apply Gauss-Hermite quadrature to efficiently approximate the integral in Equation (4) in three dimensions. Specifically, in this case, through a change of variable such that $\mathbf{L}\mathbf{L}^\top = \Sigma$ and $\mathbf{u} = \mathbf{L}^{-1}(\mathbf{x} - \mathbf{p})$, where \mathbf{L} is a lower triangular matrix computed via the Cholesky decomposition:

$$\tilde{k} = \frac{1}{(2\pi)^{\frac{3}{2}}} \sum_{i_1=1}^n \sum_{i_2=1}^n \sum_{i_3=1}^n \bar{w} k_{i_{1:3}}, \quad (5)$$

where n is the number of sample points used in the approximation, $\bar{w} \triangleq \prod_{j=1}^3 w_{i_j}$, u_{i_j} corresponds to the roots of the Hermite polynomial H_n , $\mathbf{u}_{i_{1:3}} \triangleq [u_{i_1}, u_{i_2}, u_{i_3}]^\top$, and $k_{i_{1:3}}$ is the covariance function evaluated at $\mathbf{x}_{i_{1:3}} = \mathbf{L}\mathbf{u}_{i_{1:3}} + \mathbf{p}$.

V. PLANNING APPROACH

This section overviews our informative planning scheme, which generates fixed-horizon plans through a combination of a 3-D grid search and evolutionary optimization. We summarize the key steps of the algorithm, focusing on our uncertainty-aware utility function for GP-based active mapping scenarios as the main contribution of this paper. For further details concerning the planning approach itself, the reader is referred to our previous publications [5, 15, 16].

A. Trajectories

A polynomial trajectory ψ is represented by N ordered control waypoints to visit $\mathcal{C} = [\mathbf{c}_1, \dots, \mathbf{c}_N]$ connected using $N - 1$ k -order spline segments. Given a reference velocity and acceleration, we optimize the trajectory for smooth minimum-snap dynamics [20], clamping \mathbf{c}_1 as the initial robot position. In Equation (1), $\text{MEASURE}(\cdot)$ is defined by computing the spacing of measurement sites given a constant sensor frequency and the traveling speed of the robot.

B. Algorithm

We plan using a fixed-horizon approach, alternating between replanning and execution until the elapsed time t exceeds the budget B . Our replanning strategy (Algorithm 1) consists of two steps. First, an initial trajectory is obtained through a grid search (Lines 3-7) based on a coarse set of points \mathcal{L} in the 3-D robot workspace. In this step, we conduct a sequential greedy search for N control waypoints in \mathcal{C} ; selecting the next-best point \mathbf{c}^* (Line 4) by evaluating Equation (1) over \mathcal{L} . As described in Section V-C, our new utility function (Equation (8)) defines the objective $I(\cdot)$ for planning under pose uncertainty. During this procedure, for each candidate goal, the evolution of the robot pose uncertainty Σ during travel is predicted using the SLAM back end (Line 5), as detailed in Section V-D. The result is then used to update the field model \mathcal{GP} (Line 6) and is added to the initial trajectory solution (Line 7).

Algorithm 1 REPLAN_PATH procedure

Input: Current model of the environment \mathcal{GP} , number of control waypoints N , grid points \mathcal{L} , initial position \mathbf{c}_1 , robot pose (\mathbf{p}, Σ)
Output: Waypoints defining next polynomial plan \mathcal{C}

- 1: $\mathcal{GP}' \leftarrow \mathcal{GP}; (\mathbf{p}', \Sigma') \leftarrow (\mathbf{p}, \Sigma)$ // Create local copies.
- 2: $\mathcal{C} \leftarrow \mathbf{c}_1$ // Initialize control points.
- 3: **while** $N \geq |\mathcal{C}|$ **do**
- 4: $\mathbf{c}^* \leftarrow$ Select viewpoint in \mathcal{L} using Equation (1)
- 5: $(\mathbf{p}', \Sigma') \leftarrow \text{PREDICT_MOTION}(\mathbf{p}', \Sigma', \mathbf{c}^*)$
- 6: $\mathcal{GP}' \leftarrow \text{PREDICT_MEASUREMENT}(\mathcal{GP}', \mathbf{p}', \Sigma')$
- 7: $\mathcal{C} \leftarrow \mathcal{C} \cup \mathbf{c}^*$
- 8: **CMAES**($\mathcal{C}, \mathcal{GP}, \mathbf{p}, \Sigma$) // Optimize trajectory control points.

The second replanning step (Line 8) refines the coarse grid search output. Specifically, we employ the Covariance Matrix Adaptation Evolution Strategy (CMA-ES) [21], a generic evolutionary optimization routine, to optimize the

points in \mathcal{C} by computing the information gain for a sequence of measurements taken along the corresponding trajectory. An important benefit of this approach is that the informed initialization procedure exploiting the grid-based solution effectively speeds up the convergence of the optimizer, making it suitable for online application.

C. Utility Definition

We introduce a new utility, or information gain, function $I(\cdot)$ in [Equation \(1\)](#) which considers the uncertainty of both the robot and the field map in a unified manner, without relying on any manually tuned or problem-specific parameters. The proposed formulation is suitable for mapping using a GP to represent the underlying scalar field. The main idea is to enable the robot to trade off between gathering new information and maintaining good localization. Intuitively, we expect to achieve more conservative mapping behavior compared to planning for pure information gain by encouraging new measurements to be registered at correct locations.

Our utility function discounts the information value by the robot localization uncertainty following an approach similar to that of Carrillo et al. [\[4\]](#). We develop a parallel definition for the task of monitoring a continuous field, instead of building an occupancy map. To quantify uncertainty in our field model, we leverage the definition of Rényi's entropy for a Gaussian distribution $X \sim \mathcal{N}(\mu, \sigma^2)$, given by [\[22\]](#):

$$H_\alpha(X) = \frac{1}{2} \log (2\pi\sigma^2 \alpha^{\frac{1}{\alpha-1}}), \quad (6)$$

where $\alpha \in [0, 1) \cup (1, \infty)$ is a free parameter, restricted in this work to the range $(1, \infty)$. Note that $H_{\alpha \rightarrow 1}(X) = H(X)$ converges to Shannon's entropy in the limiting case.

Applying this concept our GP field model with n points in \mathcal{X} , we measure information using Rényi's entropy with the commonly used criterion for A-optimal design [\[1, 16, 18\]](#):

$$\hat{H}_\alpha(X) = \hat{H}_\alpha(\mathbf{P}) \propto \log (\text{Tr}(\mathbf{P}) \alpha^{\frac{1}{\alpha-1}}), \quad (7)$$

where $\text{Tr}(\cdot)$ denotes the matrix trace, and the covariance matrix \mathbf{P} is obtained using the expected kernel in [Equation \(4\)](#) for mapping under uncertainty.

Our key insight is to exploit the free parameter α to scale the expected information gain from future measurements based on the localization uncertainty. For a candidate robot pose $\mathcal{N}(\mathbf{p}, \Sigma)$, we compute the mutual information between the training data of the current GP model and the new sensor observations acquired. Our utility function is defined as:

$$I_\alpha(\Sigma)(\mathbf{p}) = \hat{H}(\mathbf{P}^-) - \hat{H}_\alpha(\Sigma)(\mathbf{P}^+), \quad (8)$$

where the superscripts $-$ and $+$ denote the prior and posterior covariance matrix \mathbf{P} of the GP model, respectively.

In [Equation \(8\)](#), we relate α to the predicted uncertainty Σ , thus effectively coupling the expected information gain to potential future actions. This enables us to trade off between robot localization and field mapping in a meaningful way, without the need for any additional parameters. To capture the intuition that the information value reduces when the robot is poorly localized, we again consider a simple relationship with the A-optimal criterion as $\alpha(\Sigma) = 1 + \frac{1}{\text{Tr}(\Sigma)}$ [\[4\]](#).

D. Uncertainty Prediction

A key requirement for predictive planning is propagating the robot localization uncertainty for a candidate action (Line 5 of [Algorithm 1](#)). In unknown environments, we consider a solution to this task assuming a graph SLAM back end using odometry and point landmark observations as constraints [\[23\]](#). [Figure 2](#) schematizes a 2-D example. To predict the localization uncertainty along a possible path (dashed line), the graph is simply extended from the current pose $\mathcal{N}(\mathbf{p}_1, \Sigma_1)$. The trajectory is interpolated at a fixed frequency to add $K - 1$ odometry constraints (hollow circles) in the extended graph, giving rise to the sequence $\{\mathcal{N}(\mathbf{p}_1, \Sigma_1), \dots, \mathcal{N}(\mathbf{p}_K, \Sigma_K)\}$. For each consecutive node pair, we apply control noise drawn from a Gaussian distribution whose variance is proportional to the control input magnitude. This reflects the fact that longer motion steps are likely to be associated with higher actuation errors.

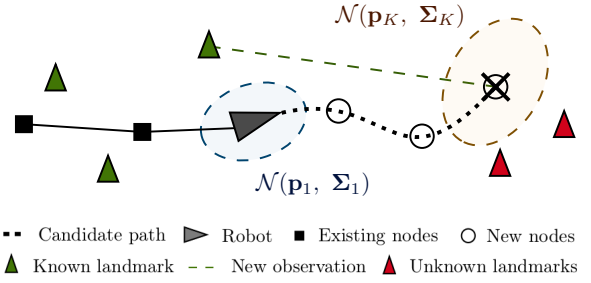


Fig. 2: Uncertainty prediction using graph SLAM with point landmarks. The dashed line is a candidate path to 'X'. Example uncertainty ellipses at initial and final positions are shown. To predict the robot pose evolution, new nodes are interpolated along the path to extend the current graph. The extended graph is optimized to estimate the final pose $\mathcal{N}(\mathbf{p}_K, \Sigma_K)$ for planning.

To address potential loop closures, we simulate re-observations to the known landmarks (green triangles) maintained in the current graph. In unknown space, we assume that no new landmarks will be detected, causing the robot pose uncertainty to grow. The resulting graph is then solved using QR factorization to obtain Σ_K . Future work will consider extending these ideas to other SLAM systems.

Similarly, in a known environment, the uncertainty can be predicted using a motion model and the expected sensor measurements obtained assuming a Monte Carlo Localization (MCL) approach. In [Section VI-C](#), this method is applied to localize a robot with a laser scanner in an indoor area.

Putting together our ideas in mapping and planning in a single framework, the GP field model with UIs accounts for the pose uncertainty in the received observations, while the proposed utility function accounts for the pose uncertainty in potential future measurements. This coupling allows us to achieve robust performance in GP-based mapping scenarios.

VI. EXPERIMENTAL RESULTS

In this section, our approach is evaluated in simulation by comparing it to different strategies for planning and mapping. We then show proof of concept by using it to map temperature using a ground robot in an indoor environment.

A. Comparison of Planning Methods

First, the aim is to evaluate our new utility function by comparing it against existing strategies. To focus on examining planning performance, all methods in this sub-section use the GP-based approach with UIs for mapping under pose uncertainty (Section IV-B). The evaluation is conducted in a simulated $5\text{ m} \times 5\text{ m} \times 4\text{ m}$ Gaussian Random Field environment. For mapping, we use a $0.25\text{ m} \times 0.25\text{ m} \times 1\text{ m}$ resolution grid and apply the isotropic squared exponential (SE) kernel with hyperparameters trained by minimizing log marginal likelihood [14]. Its modified variant in Equation (4) is estimated using Gauss-Hermite quadrature with 5 points. During a mission, field measurements are taken at 0.25 Hz using a point-based sensor centered on the robot. These are added to our GP model as observed input training points to achieve uncertainty reduction as exploration takes place.

To emulate an aerial robot setup, 10 point landmarks are uniformly placed on the ground 1 m below the target field. For SLAM, the robot is equipped with a downward-facing camera with $(47.9^\circ, 36.9^\circ)$ field of view. Our framework uses a graph SLAM back end [23] with the uncertainty prediction approach described in Section V-D for predictive planning. We sample trajectories at 0.5 Hz to simulate control actions, applying a coefficient of 0.01 in all three co-ordinate dimensions to scale the control noise variance. For planning, covariance matrices from the graph are extracted through the computations developed by Kaess and Dellaert [24].

Our Rényi-based utility function is compared against our framework using different objectives: (a) field map uncertainty reduction only (Equation (8) using standard Shannon’s entropy); (b) field map uncertainty reduction over time (rate), as in our previous works [5, 15, 16]; and (c) a linear composite of the map and pose uncertainties weighting both objectives equally based on their upper bounds [11]. As benchmarks, we also study: (d) the sampling-based rapidly exploring information gathering tree (RIG-tree) [8] and (e) random waypoint selection. A 150 s budget B is specified for all methods. To evaluate mapping performance, we quantify uncertainty with the GP covariance trace $\text{Tr}(\mathbf{P})$ and accuracy with Root Mean Squared Error (RMSE) with respect to the ground truth map. Similarly, for planning, our measures are the robot covariance trace $\text{Tr}(\Sigma)$ and the pose RMSE with respect to the ground truth trajectory. Intuitively, lower values using all metrics signify better performance.

The starting robot position is $(2\text{ m}, 2\text{ m}, 1\text{ m})$ with no prior information about the environment. For trajectory optimization, the reference velocity and acceleration are 1.5 m/s and 3 m/s^2 using polynomials of order $k = 12$. In our planner, we define polynomials with $N = 4$ waypoints and use a uniformly spaced 27-point lattice for the 3-D grid search. In RIG-tree, we associate control waypoints with vertices, and form polynomials by tracing the parents of leaf vertices to the root. The finite-horizon replanning procedure follows the approach of Popović et al. [5] with the uncertainty-only objective and a branch expansion step-size of 5 m empirically set for best performance based on multiple trials. In the

random planner, random destinations are sampled in the environment and a trajectory is generated by connecting them sequentially to the current robot position. We consider 4 waypoints per plan to ensure that the trajectory lengths are fairly comparable to our method.

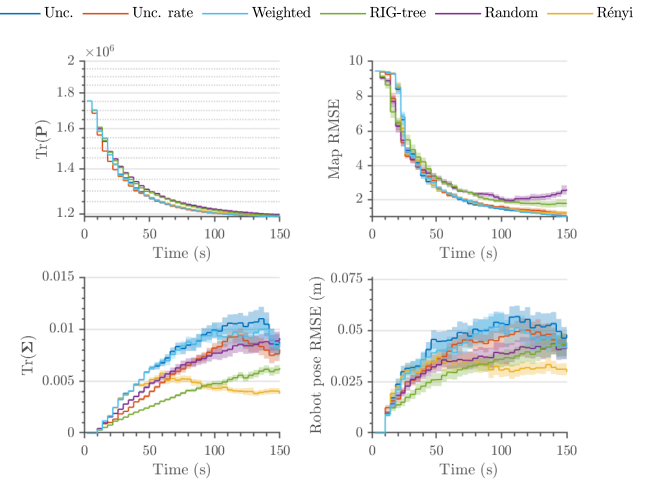


Fig. 3: Comparison of our Rényi-based utility function against planning benchmarks for a fixed budget of 150 s using GP-based mapping with UIs. The solid lines represent means over 50 trials. The shaded regions show 95% confidence bounds. By considering both the robot pose and field map uncertainties, our planner more quickly achieves higher-quality mapping (top) with improved localization (bottom). Note that $\text{Tr}(\mathbf{P})$ is on a logarithmic scale.

Figure 3 shows how the metrics evolve for each planner over the 50 trials. As expected, informed strategies perform better than the random benchmark (purple) as they are guided by planning objectives. The uncertainty-based (blue, red) and weighted (cyan) utility functions yield map uncertainty and error reduction rates similar to our Rényi-based objective (yellow). However, our method significantly improves upon the robot pose estimation in the same scenario; confirming that it effectively trades off between gathering information and maintaining good localization given the known landmarks. This cannot be done using manually tuned parameters (cyan) as the variability of the pose uncertainty is much lower compared to that of the map. In terms of localization, the uncertainty-only function (blue) performs worst as it does not exploit any knowledge of the trajectory dynamics.

Interestingly, RIG-tree (green) scores comparatively well on the localization metrics whereas the rate at which the map quality improves is limited. This likely relates to the step-size parameter required by the algorithm, which sets the range of navigation achievable during the mission. By traveling trajectories with shorter steps, the robot re-observes landmarks more frequently at the cost of restricted exploration.

An example result using our proposed utility function is shown in Figure 4. Figure 4a confirms that the robot successfully explores the environment while re-visiting known landmarks to stay well-localized. With a total RMSE of 1.11, the map output in this instance (Figure 4b) is 1.86 times more accurate than the one produced by the naïve spiral path in Figure 1, thus justifying our informative planning strategy.

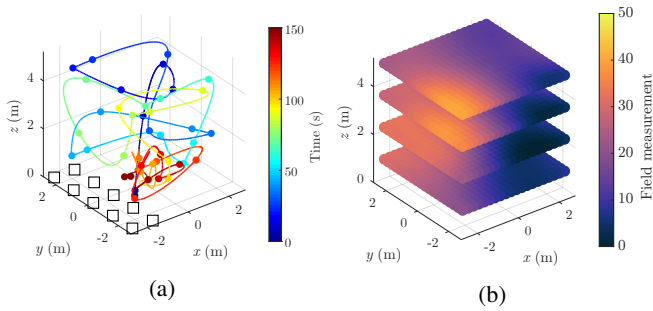


Fig. 4: Example result using our Rényi-based utility function. (a) shows the trajectory traveled by the robot. The squares indicate point landmarks used for localization. The spheres represent sites where measurements are taken to produce the final field map in (b). By balancing between gathering new information and keeping the landmarks in view, our planner achieves 1.86 lower total field map RMSE compared to the spiral path shown in Figure 1.

B. Evaluation of Field Mapping Under Uncertainty

Next, the aim is to assess the benefits of mapping under the robot pose uncertainty by evaluating the effects of incorporating UIs in the GP field model. We consider the same simulation setup as described above using our proposed Rényi-based utility function for planning. We conduct 50 trials each (a) with and (b) without applying the modified kernel presented in Section IV-B. Note that (b) corresponds to a standard GP mapping approach as a benchmark.

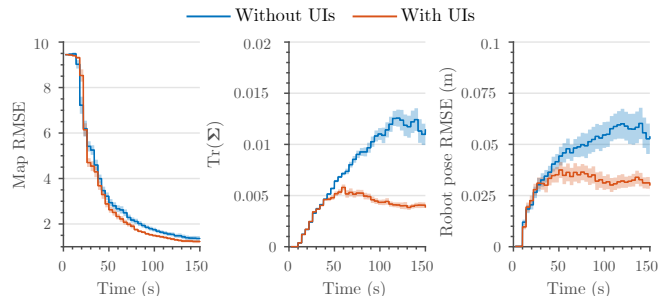


Fig. 5: Comparison of field mapping with and without uncertain inputs (UIs) using our Rényi-based utility function for a fixed budget of 150 s. The solid lines represent means over 50 trials. The shaded regions show 95% confidence bounds. By accounting for the robot pose uncertainty, our approach achieves more conservative mapping behavior (middle, right) with higher accuracy (left).

Our results are depicted in Figure 5. Note that we omit the map uncertainty metric as the variance scales using the two approaches are not comparable. The plots confirm that our approach with UIs (red) presents more conservative exploratory behavior than the benchmark (blue) while also yielding more accurate field reconstructions. This is because our modified kernel can handle localization errors to build maps with better consistency and quality for reliable planning. Figure 1 shows a visualization that supports this result.

C. Proof of concept

We show our active sensing framework running in real-time on a TurtleBot3 Waffle with an Intel Joule 570x running Ubuntu Linux 16.04 and the Robot Operating System. The

experiments are conducted in a known indoor environment using Adaptive Monte Carlo Localization (AMCL)¹ receiving data from a LDS-01 laser distance scanner. As shown in Figure 6b, for field mapping, a temperature distribution in an empty 2.8 m × 2.8 m area within the environment is generated using a 2400 W radiant heater placed at one corner. Measurements are taken using a LM35 linear temperature sensor with a sensitivity of 10 mV/°C.

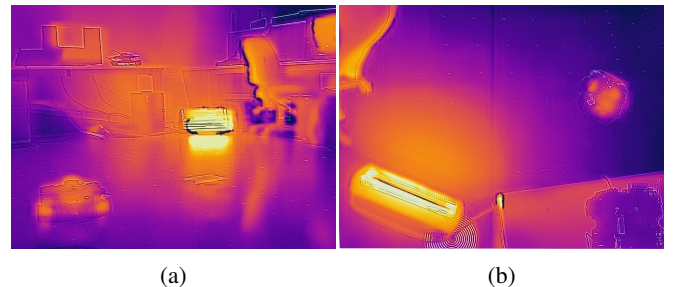


Fig. 6: Thermal imagery of our experimental setup from side (a) and aerial (b) viewpoints. The robot and radiator are visible. Yellower shades correspond to heated areas mapped using measurements from the on-board temperature sensor.

A 0.4 m resolution grid is set for mapping with UIs. To train the GP, we follow the method in Section VI-B using manually gathered data within the target area to obtain the hyperparameters for the SE kernel. As before, the integral in Equation (4) is estimated using 5 Gauss-Hermite points.

Our uncertainty prediction method is based on localization in a known environment using AMCL (Section V-D). We sub-sample each candidate plan at 2 Hz and estimate the robot pose using a differential drive odometry model and laser scans simulated in the known occupancy map. For the odometry model, variance parameters of 0.2 m² are used for Gaussian noise in both rotational and translational motion.

The aim is to show that our framework can map a realistic continuous field using a practical localization system. The initial measurement point is (0.2 m, 0.2 m) within the corner opposite the radiator. We allocate a planning budget B of 600 s. Following the differential drive model, each plan is piecewise linear as defined by $N = 3$ control waypoints with a constant velocity of 0.26 m/s and temperature measurements sampled at 0.25 Hz. The planning objective is our proposed Rényi-based utility function in Equation (8). Note that field map updates are triggered upon allowing the sensor readings to stabilize between successive measurement points.

Figure 7 summarizes our experiments. As expected, the field map becomes more complete over time and uncertainty decreases as the yellower heated region is discovered in a successful proof of concept implementation. Note that the mean value of the GP is lower than the range of measurements obtained due to the effects of heating and diffusion making it difficult to obtain a controlled temperature field as a reference. This motivates addressing temporal dynamics as a potential direction for future work.

¹wiki.ros.org/amcl

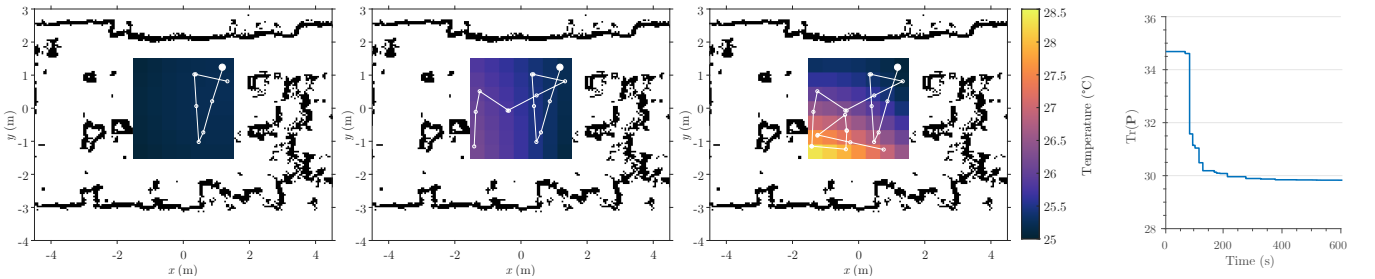


Fig. 7: Experimental results of using our active sensing framework to map the indoor temperature distribution in Figure 6 in a 600 s mission. The three plots on the left depict the trajectories (white lines) and temperature field maps (colored gradients) at different snapshots of the mission at times $t = 100$ s, 350 s, and 600 s. The white circles represent measurement sites, with the large solid one indicating the initial robot position. Yellower shades correspond to hotter regions. The sequence shows that our planner quickly explores the area, successfully detecting the heated corner (bottom-left) where the radiator is located. The curve on the right shows the uncertainty reduction in the field map over time, thus validating our approach. Note that planning time is taken into account.

VII. CONCLUSIONS AND FUTURE WORK

This work introduced an informative planning framework for active mapping that accounts for the robot pose uncertainty in both the mapping and planning stages. Our method uses GPs with UIs to propagate the robot pose uncertainty into the model of a target environmental field. For planning, we introduced a new utility function that tightly couples the uncertainties in the robot pose and field map by applying the concept of Rényi's entropy in GP-based mapping scenarios. Our formulation enables the robot to trade off between exploration and exploitation in a principled way, without relying on any manually tuned parameters.

Our framework was evaluated extensively in simulation. We showed that it achieves more conservative exploratory behavior compared to different planning and mapping strategies, while producing more accurate maps. Experimental validation was performed through a proof of concept deployment, revealing its promise in future applications.

Future work will examine field models with temporal dynamics and efficiency improvements to handle more complex environments. Other interesting research directions involve refining the uncertainty prediction method and its relationship to the Rényi parameter α for more reliable planning.

REFERENCES

- [1] G. Hitz, E. Galceran, M.-È. Garneau, F. Pomerleau, and R. Siegwart, “Adaptive Continuous-Space Informative Path Planning for Online Environmental Monitoring,” *Journal of Field Robotics*, vol. 34, no. 8, pp. 1427–1449, 2017.
- [2] M. G. Jadidi, J. V. Miro, and G. Dissanayake, “Sampling-based Incremental Information Gathering with Applications to Robotic Exploration and Environmental Monitoring,” 2016.
- [3] R. Oliveira, L. Ott, V. Guizilini, F. Ramos, and R. O. Sep, “Bayesian Optimisation for Safe Navigation under Localisation Uncertainty,” in *International Symposium of Robotics Research*. Puerto Varas: Springer, 2017.
- [4] H. Carrillo, P. Dames, V. Kumar, and J. A. Castellanos, “Autonomous robotic exploration using a utility function based on Rényi's general theory of entropy,” *Autonomous Robots*, vol. 42, no. 2, pp. 235–256, 2018.
- [5] M. Popović, T. Vidal-Calleja, G. Hitz, J. J. Chung, I. Sa, R. Siegwart, and J. Nieto, “An informative path planning framework for UAV-based terrain monitoring,” *Autonomous Robots*, 2019, under review, arXiv preprint [arXiv:1809.03870](https://arxiv.org/abs/1809.03870).
- [6] C. Papachristos, S. Khattak, and K. Alexis, “Uncertainty-aware Receding Horizon Exploration and Mapping using Aerial Robots,” in *IEEE International Conference on Robotics and Automation*. Singapore: IEEE, 2017, pp. 4568–4575.
- [7] S. Manfreda, M. F. McCabe, P. E. Miller, R. Lucas, V. P. Madrigal, G. Mallinis, E. B. Dor, D. Helman, L. Estes, G. Ciraolo, J. Müllerová, F. Tauro, M. I. de Lima, J. L. de Lima, A. Maltese, F. Frances, K. Caylor, M. Kohv, M. Perks, G. Ruiz-Pérez, Z. Su, G. Vico, and B. Toth, “On the Use of Unmanned Aerial Systems for Environmental Monitoring,” *Remote Sensing*, vol. 10, no. 4, 2018.
- [8] G. A. Hollinger and G. S. Sukhatme, “Sampling-based robotic information gathering algorithms,” *International Journal of Robotics Research*, vol. 33, no. 9, pp. 1271–1287, 2014.
- [9] A. Girard, “Approximate methods for propagation of uncertainty with Gaussian process models,” Ph.D. dissertation, University of Glasgow, 2004.
- [10] A. Mchutchon and C. E. Rasmussen, “Gaussian Process Training with Input Noise,” *Advances in Neural Information Processing Systems*, pp. 1341–1349, 2011.
- [11] F. Bourgault, A. A. Makarenko, S. B. Williams, B. Grocholsky, and H. F. Durrant-Whyte, “Information Based Adaptive Robotic Exploration,” in *IEEE/RSJ International Conference on Intelligent Robots and Systems*. Lausanne: IEEE, 2002, pp. 540–545.
- [12] R. Valencia, J. V. Miró, G. Dissanayake, and J. Andrade-Cetto, “Active Pose SLAM,” in *IEEE/RSJ International Conference on Intelligent Robots and Systems*, Vilamoura, 2012, pp. 1885–1891.
- [13] S. D. Whitehead and D. H. Ballard, “Active Perception and Reinforcement Learning,” *Neural Computation*, vol. 2, no. 4, pp. 409–419, 2008.
- [14] C. E. Rasmussen and C. K. I. Williams, *Gaussian Processes for Machine Learning*. Cambridge, MA: MIT Press, 2006.
- [15] M. Popović, G. Hitz, J. Nieto, I. Sa, R. Siegwart, and E. Galceran, “Online Informative Path Planning for Active Classification Using UAVs,” in *IEEE International Conference on Robotics and Automation*. Singapore: IEEE, 2017.
- [16] M. Popović, T. Vidal-Calleja, G. Hitz, I. Sa, R. Y. Siegwart, and J. Nieto, “Multiresolution Mapping and Informative Path Planning for UAV-based Terrain Monitoring,” in *IEEE/RSJ International Conference on Intelligent Robots and Systems*. Vancouver: IEEE, 2017.
- [17] L. Kaelbling, M. Littman, and A. Cassandra, “Planning and Acting in Partially Observable Stochastic Domains,” *Artificial Intelligence*, vol. 101, no. 1-2, pp. 99–134, 1998.
- [18] G. Costante, J. Delmerico, M. Werlberger, and P. Valigi, “Exploiting Photometric Information for Planning under Uncertainty,” in *Robotics Research*. Springer, 2017, pp. 107–124.
- [19] A. Bry and N. Roy, “Rapidly-exploring random belief trees for motion planning under uncertainty,” in *IEEE International Conference on Robotics and Automation*. Shanghai: IEEE, 2011, pp. 723–730.
- [20] C. Richter, A. Bry, and N. Roy, “Polynomial Trajectory Planning for Aggressive Quadrotor Flight in Dense Indoor Environments,” in *International Symposium of Robotics Research*. Singapore: Springer, 2013.
- [21] N. Hansen, “The CMA evolution strategy: A comparing review,” *Studies in Fuzziness and Soft Computing*, vol. 192, no. 2006, pp. 75–102, 2006.
- [22] L. Golshani and E. Pasha, “Rényi entropy rate for Gaussian processes,”

- Information Sciences*, vol. 180, no. 8, pp. 1486–1491, 2010.
- [23] J. Solà, “Course on SLAM,” Barcelona, 2017.
- [24] M. Kaess and F. Dellaert, “Covariance recovery from a square root information matrix for data association,” *Robotics and Autonomous Systems*, vol. 57, no. 12, pp. 1198–1210, 2009.